High Velocity Impact Performance of a Dual Layer Thermal Protection System for the Mars Sample Return Earth Entry Vehicle

B.J. Libben[1], J.T. Needels[2], D.T. Ellerby[3], J.C. Vander Kam[3], T.R. White[3], P.J. Gage[2], D.K. Robertson[3], A.M. Coates[3]

[1]AMA Incorporated at NASA Ames Research Center, USA
[2]Neerim Corporation at NASA Ames Research Center, USA
[3]NASA Ames Research Center, USA

1 MOTIVATION

The Mars Sample Return (MSR) Campaign is a multi-mission effort with the overall objective of robotically collecting samples of regolith from the Martian surface and returning them to Earth for examination. Due to planetary protection concerns associated with loss of sample containment, the MSR Earth Entry Vehicle (EEV) is expected to carry unprecedented reliability requirements, which flow down to all sub-systems, including the thermal protection system (TPS).

Performance of TPS in an off-nominal state due to hypervelocity micrometeoroid/orbital debris (MMOD) impact has been identified as a primary risk driver for the MSR EEV. The EEV will be released from its shielded housing approximately five days prior to entry interface during the Earth return trajectory, leaving it exposed to the space environment for the remainder of the cruise. Of particular concern is impact damage to the ablative forebody heat shield, which will encounter extreme aerothermal environments during Earth entry. Bondline temperature, the temperature at the adhesive interface of the Inner Mold Line (IML) of the TPS and the EEV structure, is the primary figure of merit for TPS. Exceeding limitations on bondline temperature over a sufficiently large area can result in structural failure of the EEV, potentially leading to sample non-containment. Detailed understanding of TPS material performance under hypervelocity impact damage is necessary to accurately quantify risk in support of TPS selection.

An overview of TPS hypervelocity impact (HVI) risk assessment is given in Fig 1 below. Current standard practice for modeling hypervelocity impact damage to space vehicles is the application of Ballistic Limit Equations (BLEs). BLEs predict penetration depth as a function of projectile mass and velocity, as well as projectile and target material properties. The close coupling between impact crater geometry and the local aerothermal environment differentiates assessment of TPS impact risk from other space vehicles. Damage progression modes can result in unacceptably elevated bondline temperatures for impact craters that do not penetrate all the way through the TPS. Coupled fluid/thermal analyses have demonstrated that aerothermal environments in the vicinity of a crater are sensitive to crater morphology, which is not captured in the material BLE.

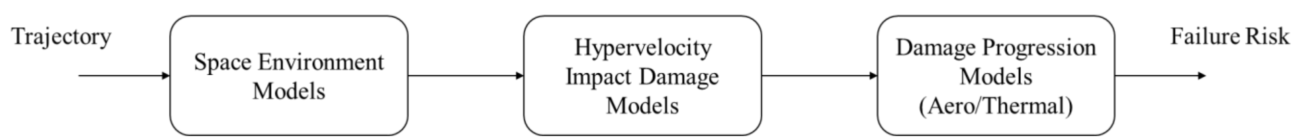

Fig 1. HVI Risk Assessment Process for MSR EEV

At present, two materials are candidates for the MSR EEV forebody heat shield: Heat shield for Extreme Entry Environments Technology (HEEET), a dual layer material composed of three-dimensionally woven carbon yarn impregnated with low density phenolic resin, and Phenolic Impregnated Carbon Ablator (PICA), a homogenous carbon tile material impregnated with low density phenolic resin. PICA is a heritage TPS material selected for several missions, including Stardust, Mars Science Laboratory, OSIRIS-Rex, and the soon to be flown Mars 2020 mission. From previous testing conducted during the Orion program, PICA has been well characterized for impacts representative of orbital debris (high density, low velocity projectiles), but has not undergone extensive micrometeoroid impact testing.

HEEET is a recently developed material, assessed to be at Technology Readiness Level 6 in 2019 [1], with limited hypervelocity test data available. While HEEET was developed as a dual layer TPS with a high density Recession Layer (RL) on top of a lower relative density Insulation Layer (IL), as shown in Fig. 2, recent arc jet testing has demonstrated sufficient aerothermal capability of the IL alone. Modeling of an IL only heat shield entering in MSR EEV expected aerothermal environments has shown that a Single Piece IL (S/IL) heat shield design can close from both an aerothermal and mass perspective. The difference in density between HEEET IL and RL, 0.83 g/cm^3 compared to 1.1 g/cm^3 respectively, makes an IL-only heat shield attractive from a mass efficiency standpoint. However, differences in hypervelocity impact performance between IL only and dual layer HEEET, as well as any impact performance benefit from increasing RL thickness, are not well understood.

In order to accurately assess hypervelocity impact risk to TPS samples, and discriminate residual risk between candidate architectures, an engineering test program was developed to better understand TPS HVI material response and crater morphology. The FY19 HVI Test (HVIT) series included three different RL/IL layer ratios of HEEET to be tested alongside heritage PICA to characterize response of the dual layer material relative to a heritage baseline, as well as to determine the marginal effect of RL thickness on material HVI performance. Computed Tomography (CT) scans of test coupons were analyzed and compared against hydrocode simulation results outlined in section 4.1, to better understand the effect of material and impactor parameters on the morphology of the resulting craters.

Fig. 2. Anatomy of Heatshield for Extreme Entry Environment Technology (HEEET).

2 ENVIRONMENT RISK CHARACTERIZATION

Due to the short exposure time of the TPS in the orbital debris environment relative to the micrometeoroid environment, hypervelocity impact risk for MSR EEV is driven by micrometeoroid impact [2]. Analysis of impact risk involves characterization of the meteoroid environment along the EEV trajectory, as well as mapping the resulting distributions of particle fluxes and velocities to the EEV surface.

2.1 Meteoroid Environment Analysis

The primary tool used to characterize the meteoroid environment is the NASA Meteoroid Engineering Model (MEM), developed by the Meteoroid Environment Office (MEO) at NASA Marshall Space Flight Center (MSFC). MEM computes a directional distribution of meteoroid flux and particle velocity as a function of vehicle trajectory. These results can then be input into a ballistic risk evaluation program, such as the Bumper [3] tool, which maps the flux distribution to the vehicle surface and determines risk of impact.

2.2 Ballistic Impact Damage Analysis

Bumper is the primary MMOD risk analysis tool used by NASA, and is configuration controlled by the Hypervelocity Impact Technology Group (HVITG) at NASA Johnson Space Center (JSC). Bumper maps directional flux and velocity distributions produced by a space environment model to a particular vehicle geometry, using a library of material response models in order to predict damage from a given MMOD impact [4]. Figure 3 displays results from Bumper analysis, showing total number of impacts per area and the consequent probability of bondline penetration due to micrometeoroids for the EEV heat shield.

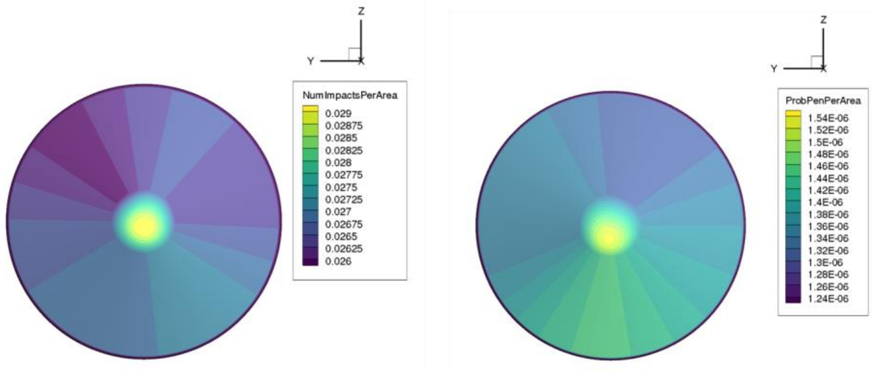

Fig. 3. Bumper Analysis of 4 Day EEV Free Flight Trajectory. All values are m^{-2}.

In addition to Bumper predictions, a development effort was undertaken at NASA Ames Research Center (ARC) to develop low fidelity risk assessment capabilities for fast-turn around preliminary design. The Ablative Material Ballistic Evaluator (AMBER) is used primarily for first order sensitivity analysis to variations in TPS material and space environment. AMBER was verified against the Bumper tool for select test cases along the MSR trajectory, and produced prediction impacts within ±3% of the Bumper values.

2.3 Volume Analysis and Comparison with Blast Wave Theory

BLEs are semi-empirical, with material specific coefficients informed by experimental data; however, the form of the equation is informed by theoretical models of shock wave propagation in homogenous media. Blast Wave Theory is a mathematical model for a radially expanding spherical shock wave, and forms the basis for many ballistic limit equations.

An assumption implicit to BLEs based on Blast Wave Theory, such as the HEEET BLE, is that volume of the resulting impact crater is proportional to the kinetic energy of the projectile, and impacts in semi-infinite homogeneous materials are well described by such models [6]. However, there is concern that the BLE does not adequately model impact energy accommodation in a dual-layer, three-dimensionally woven material, such as HEEET, and therefore may not be predictive when extrapolated beyond the regime of test capabilities.

2.4 Monte Carlo

To characterize the MSR EEV expected micrometeoroid environment, the micrometeoroid velocity distribution output by MEM for the MSR EEV trajectory (Fig. 4) and the mass distribution model from NASA TM 4527 [5] were used to run a 10 million point Monte Carlo simulation of the expected mass and velocity combination of expected EEV impacts. The Monte Carlo results were then binned into a 2D histogram in Fig. 5 (a) to determine the probability density for the varying impact parameter combinations.

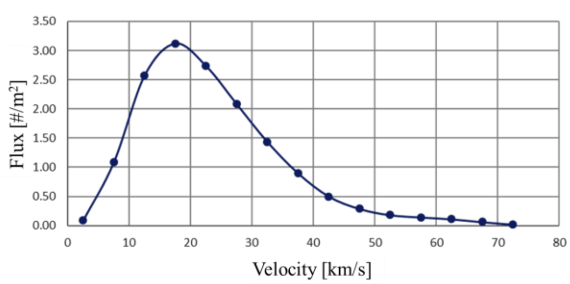

Fig. 4: Velocity Distribution output from MEMR2 for a notional 3 day trajectory.

Since the expected impactor (~25 km/s and 1e-6 g) is far out of the testable range of current ground facilities, a way to extrapolate HVI testing out to these predicted projectiles is needed. As stated in section 2.3, Blast Wave Theory predicts that at a constant Kinetic Energy, an impactor's crater volume will remain constant. This assumption allows the testing of relatively high mass projectiles at low velocities – equating to a predicted particle's kinetic energy – to inform TPS material performance against those expected impacts.

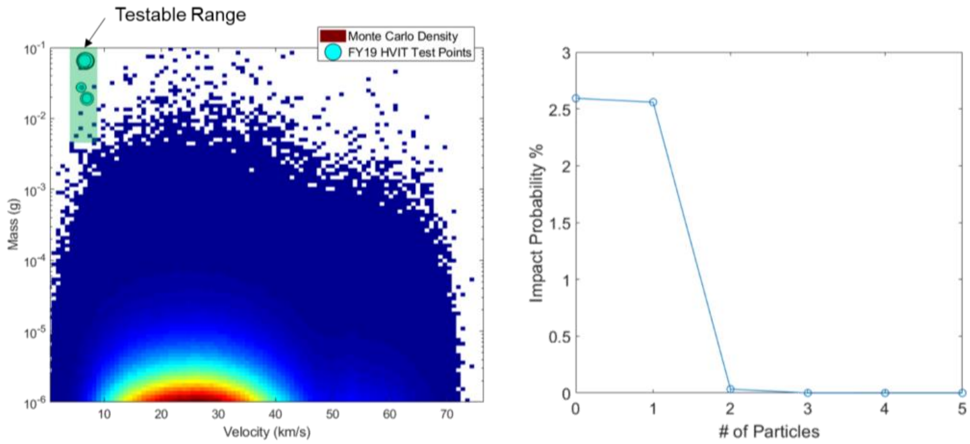

(a) (b)

Fig. 5: (a) 2D Histogram of the Monte Carlo results with contours of impactor parameter combination density. Since the testable range is unrepresentative of the expected impactors, extrapolations of ground testing are done through testing constant kinetic energy levels. (b) Poisson distribution of the probability the MSR-EEV will experience a number of impacts. These two results are combined to determine the probability of the vehicle being impacted by a specific kinetic energy.

Since Fig. 5 (a) only represents the parameter probability density of the case where the vehicle is impacted, the probability of an impact event occurring during the mission needs to be determined. This impact probability can then be multiplied by the probability density of impactor parameter combinations to determine the overall probability of the EEV being impacted by a specific kinetic energy level. Using a Poisson distribution on the MEM predicted ram flux in Fig. 5 (b), the probability that the EEV experiences an HVI is ~2.5%. The kinetic energies for increasing magnitudes of impact probability can be calculated, and the 1e-6 impact energy for the EEV trajectory, shown in red in Fig. 6, can be determined. This energy level signifies the limit of kinetic energies the EEV's forebody TPS would need to protect against to maintain at least a 1e-6 probability risk posture for MMOD events.

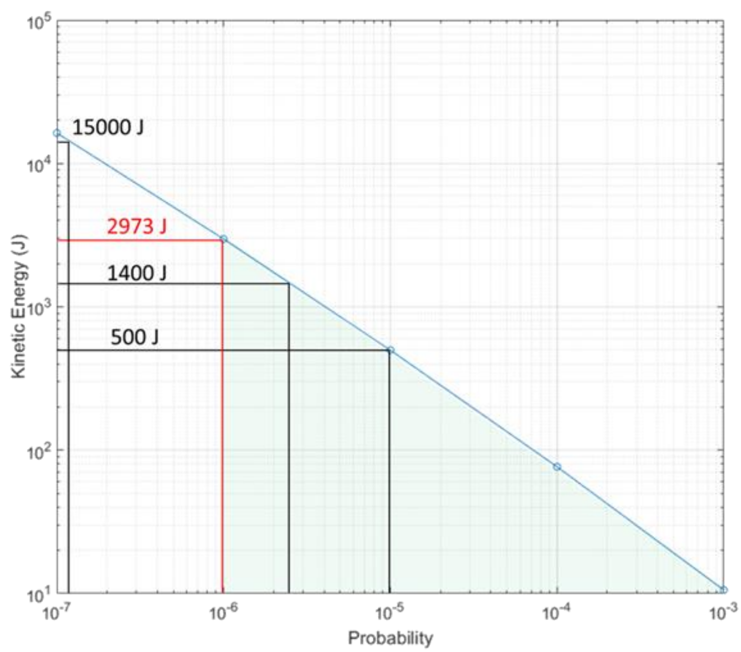

Fig. 6: Kinetic energy probabilities for a 5-day MSR-EEV flight trajectory. The black kinetic energy levels represent the FY19 HVI test series nominal conditions, and the red energy represents the 1e-6 probability particle.

3 HYPERVELOCITY IMPACT TEST PROGRAM

Hypervelocity testing was conducted using the two-stage light gas guns (LGGs) at NASA White Sands Test Facility (WSTF). The LGGs at WSTF are limited in the range of projectile mass and velocities at which they can test, and have been primarily driven by Low Earth Orbit (LEO) mission requirements where orbital debris is the primary risk driver. Ground test velocities are limited to between ~5-8 km/s (highlighted green in Fig. 5), well below the average expected meteoroid impact velocity of ~25 km/s. Since this testable range does not well represent the expected micrometeoroid environment, a method to extrapolate ground testable shots out to actual expected parameters is needed. Blast Wave Theory assumes that crater volume remains constant with a constant kinetic energy despite the change in crater topology. This allows the use of kinetic energy as the control parameter to extrapolate material performance outside of the testable range. Table 1 outlines the test series primary objectives, with this paper focusing primarily on Objective 1.

Table 1. MSR EEV FY 19 Hypervelocity Impact Test Objectives

1. The test program shall assess the incremental benefit of increasing RL thickness on MM impact performance
2. Test program projectile densities shall be representative of the meteor environment
3. The test program shall assess the full range of anticipated impact angles
4. The test program shall assess the difference in material response between HEEET and PICA for similar impact energies, impact angles, and impact densities
5. The test program shall assess the MM impact performance of thermally sized PICA bonded to a flight-representative composite sub-structure

A summary of the test program parameters is given in Table 2 below. A fractional factorial test matrix was developed, based on the test objectives above, constrained by cost, schedule, and material availability.

Table 2. Summary of Test Program Parameters

Factor	Variants			
Backing	0.04" Composite Facesheet		0.375" Al Plate	
Target Material	5 – 13.3 cm [2– 5.35 in] thick PICA	3.18 cm [1.25 in] thick HEEET IL	3.18 cm [1.25 in] thick HEEET 0.13 cm [0.05 in] RL	3.18 cm [1.25 in] thick HEEET 0.26 cm [0.1in] RL
Projectile Material	Nylon		Aluminum	
Impact Angle	0 degree		70 degree	
Energy	Low Energy 500 Joules ~1/100,000 likelihood for 5 days of free-flight		High Energy 1400 Joules ~4/1,000,000 likelihood for 5 days of free-flight	

In order to understand the effect of increasing RL thickness on dual-layer HEEET impact performance, two different RL thickness samples were prepared and compared to IL only HEEET. These samples in turn were compared to various thickness samples of PICA.

All HEEET test samples were mounted on 3/8” thick aluminum plates to match testing done on PICA during the Orion program. PICA samples in this test series were bonded to either 3/8” aluminum plate or 0.04” composite facesheets.

In order to satisfy the second test objective, two different projectile densities were tested. The meteoroid distribution is bi-modal, with a larger peak at ~1 g/cm^3 and a smaller peak at ~3.6 g/cm^3. To approximate low density impactors, nylon projectiles were used, with nominal density 1.14 g/cm^3. The high density meteoroid population was approximated by aluminum, with nominal density 2.796 g/cm^3, which though lower than the mean of the high density population, provide a useful comparison between the characteristics of high and low density impacts.

Projectile velocity was selected based on the kinetic energy contours shown in Fig. 5. Two energy levels were selected, 500 J and 1400 J, corresponding to full penetration of bounding TPS thicknesses for a preliminary three day free flight trajectory. Due to kinetic energy being held constant when testing this difference, however, the nylon and aluminum particles will have different diameters which will inflate the difference in crater size between the two materials due to the BLE dependency on impactor diameter.

While normal impacts are typically considered bounding from a penetration depth standpoint, Computational Fluid Dynamics (CFD) analysis concludes that oblique HVIs potentially pose higher risk from an aerothermal standpoint. Two different impact angles, 0 and 70 degrees, were used to better determine sensitivity of the resultant crater shape on this parameter.

4 FY19 HVI TEST RESULTS

4.1 Hydrocode Results

Hydrocode is a computational tool used to model the behaviour of fluid-like media. Since Blast Wave Theory dictates that a solid material performs like a liquid when impacted at high velocities, hydrocodes can be used to simulate the effects of an impact on the EEV’s TPS. Simulation of hypervelocity impact craters was conducted at NASA ARC in parallel with the HVI testing conducted at NASA WSTF. The Ale3D [7] code developed by Lawrence Livermore National Laboratory was used to simulate material response to hypervelocity impact, using material and projectile parameters informed by the HVI test matrix. Impact craters were simulated in both HEEET variants and PICA using a variety of boundary conditions. A simulated crater is shown compared to the FY19 HVI test article CT scan in Fig. 7. Ale3D simulations will be anchored to the FY19 HVI test results and used alongside the constant volume assumption outlined in section 2.4 to predict impactor damage to a given TPS design.

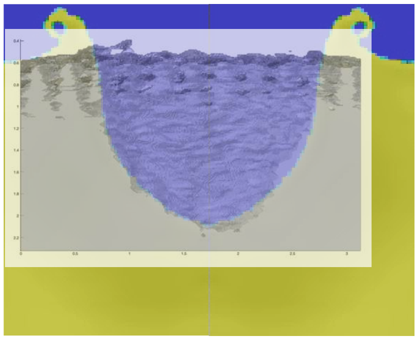

Fig. 7. Ale3D Simulation of Hypervelocity Impact in IL Only HEEET overlaid on an actual CT scan of an FY19 HVI test crater.

4.2 The Effect of HEEET Recession Layer Thickness on Crater Morphology

The first objective in the FY19 HVIT test series was to assess the variation in material performance as the Recession Layer (RL) increased in thickness. This was done by including three different thicknesses of RL on a fixed IL thickness, ranging from 0 to 0.1”. Coupons were fabricated by taking a nominally woven 0.5” RL infused HEEET panel – 1.8” in total thickness with the Insulation Layer – and machining the RL down to the required thickness. Consequently, all coupons had the same thickness of Insulation Layer (within the tolerances of machining) and varying total thicknesses. To inform the current predictive capabilities of particle penetration depth, the HVIT crater depth measurements were also compared to the as-shot parameter BLE results.

Measurements of each crater's depth and minor/major axis entry diameters were performed in two ways: JSC optical laser measurements and ARC CT scan measurements. CT scan measurements have the advantage of a much higher resolution, and more accurate results in depth of the craters; these reasons led to the CT scan data being used in the final analysis.

The first takeaway when looking at the penetration depth data in Fig. 8 is the noticeable lack of decreasing crater depth with increasing the RL thickness over the tested range. There are even a few cases where the performance seems to degrade when adding an RL layer. To see if this trend continues into large RL thicknesses, data from a limited HVI test series performed on ~0.5" RL thickness HEEET samples in FY18 was included in Fig. 9. It is clear that there is an overall gain in performance when looking at penetration depth differences in IL only and nominally woven 0.5" thickness RL samples, however, this performance increase is limited. The resulting conclusion is that marginal increase in RL thickness is not an effective method of mitigation of MMOD HVI damage, and that IL only is the most mass efficient version of HEEET with regards to impact risk.

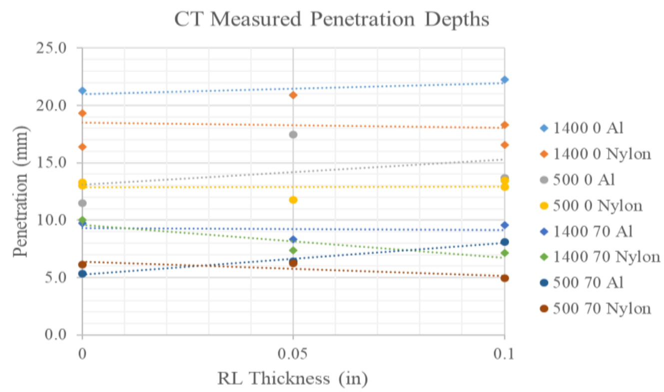

Fig. 8. CT measured penetration depths versus nominal HEEET RL thickness. Legend parameters are organized as nominal kinetic energy, impact angle, and particle material. As expected, normal impacts are grouped at the top, with both impact angles having larger penetration depths at higher energy.

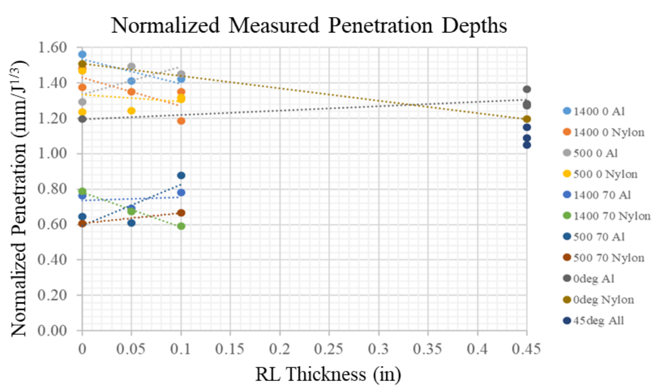

Fig. 9. FY18 and FY19 HEEET HVIT penetration data plotted as a function of increasing RL thickness. FY18 shots were all conducted on nominal 0.5" RL samples. Penetration depth was normalized with regards to the cube root of impactor energy (due to the relationship between depth and energy in Blast Wave Theory) due to the differences in FY18 and FY19 as-shot kinetic energies.

4.3 BLE Prediction Accuracy

The current BLE's generated for Bumper analysis come out of limited 0.5" RL thickness FY18 HVI optical measurements in Fig. 9. Since these equations are the state-of-the-art method to predict penetration depth, it is important to understand the inherent error when evaluating the EEV's risk potential. Both the optical and CT scan reported depth measurements were compared to the HEEET BLE in Fig. 10 to inform the proper method to predict the EEV TPS robustness, and the margin of error in said predictions.

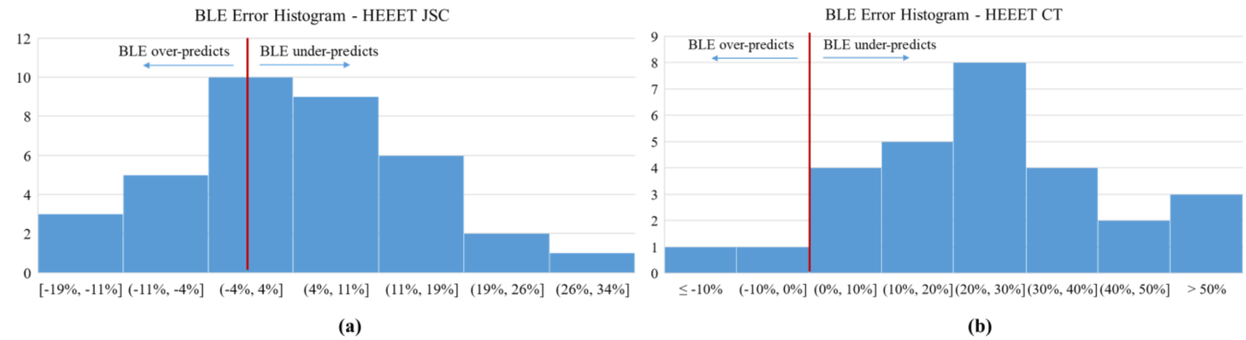

Fig. 10. (a) Histogram of BLE penetration error when predicting the as-shot HVIT series parameters to the optical measured depths (b) Histogram of BLE penetration error when predicting the as-shot HVIT series parameters to the CT scan measured depths

As expected, the HEEET BLE better predicted the optical measurements of the FY19 crater depths. Since the method of taking data to form the BLE was the same as the method to compare the BLE against, a normal distribution centered on zero error shows that the BLE was statistically well formed based on the experimental data supplied. When performing the same as-shot parameter BLE predictions against the CT scan measured depth, a normal distribution also appears, but is shifted greatly to the right with a mean error around a 25% BLE under-prediction of depth. Looking at an example CT scan of an FY19 HVIT crater in Fig. 11, it is apparent that the optical measurements are not able to capture the "finger" features consistently found at the bottom of HEEET HVI craters. Despite these features not being predicted by Blast Wave Theory, and subsequently not captured in BLE predictions, it is important for the MSR EEV team to include these features in depth reports to properly size TPS thickness to MMOD risk levels. As a result, the HVITG at JSC took FY19 CT scan depth measurements to form an updated HEEET IL BLE for future penetration predictions.

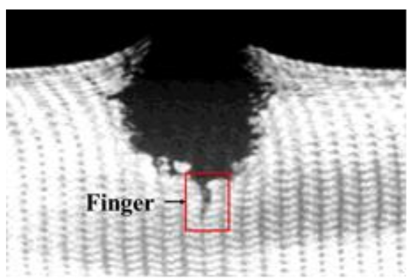

Fig. 11. Cross-section view of an FY19 HEEET HVIT crater. Optical measurements would only be able to capture the general spherical portion of the crater, while CT scans allow the "finger" features commonly seen in HEEET post-test craters to be included in depth measurements.

4.4 Inspection and Mesh Processing Algorithm for CT scans - IMPACT

To further analyze the topology of HVIT craters, actual crater geometries can be imported into a geometric mesh to support measurement of crater volume and area. Traditionally, this would be done with a laser scan of the crater, generating point cloud data that could ultimately be meshed to form a surface. Laser scanning, as previously mentioned, does not have the capability of capturing all features seen in a HEEET impact crater. Additionally, frayed fibers along the crater walls can result in laser scattering, introducing errors and increasing the overall uncertainty of the captured data. To this effect, the Inspection and Mesh Processing Algorithm for CT scans (IMPACT) code was written, and its place in the process of creating mesh data is displayed in Fig. 12.

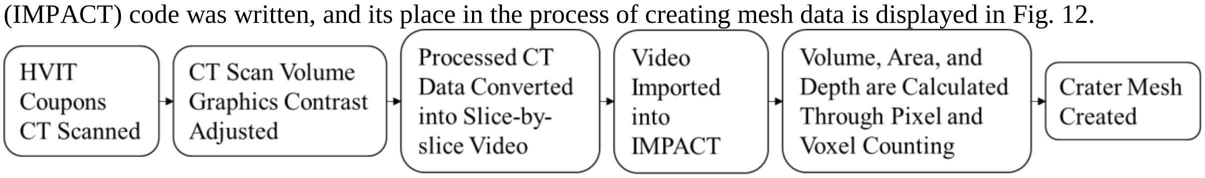

Fig. 12. Crater analysis flow chart.

Figure 13 displays the exported mesh from IMPACT processing. HEEET is a more complex material to process due to the variation in densities between the blended yarn weave and infused phenolic resin. IMPACT smooths the video frame images to blend these density variations, but in some areas the image processing cannot completely remove them – especially in lower density IL – and “bubbles” seen in the left image in Fig. 13 form in the mesh. This is generally not an issue for further use of the meshes such as true crater CFD simulation, but does add error (<1%) in the reported areas and volume.

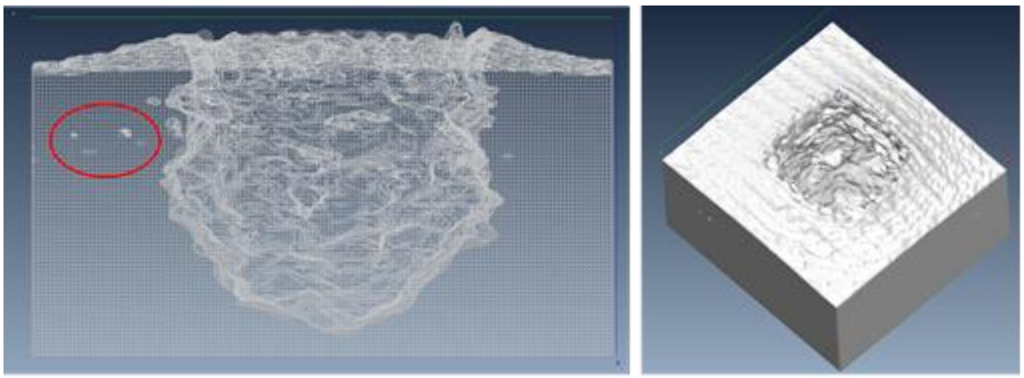

(a) (b)

Fig. 13. (a) Side-Wireframe view of an IMPACT outputted mesh with bubbles in red (b) Surface view of an IMPACT outputted mesh

4.5 Qualitative Analysis of Post-Test Coupons

As noted in the previous section, one of IMPACT’s main outputs is slice by slice area calculations as you move through the thickness of the TPS material. Fig. 14 is an example of these calculations for both a 0.1” RL and IL only coupon. Coupons with a recession layer on top consistently show two peaks of high area in-depth of the crater. This would either point to a “bunker-buster” type crater, or the RL not being incinerated as easily during initial impact. Comparatively, IL only coupons show a steady decrease in cross-sectional area as the hole gets deeper, with the largest area being at the Outer Mold Line (OML) of the TPS. While the typical crater shape differences are interesting, there does not seem to be any noticeable effect on penetration depth, and therefore TPS risk.

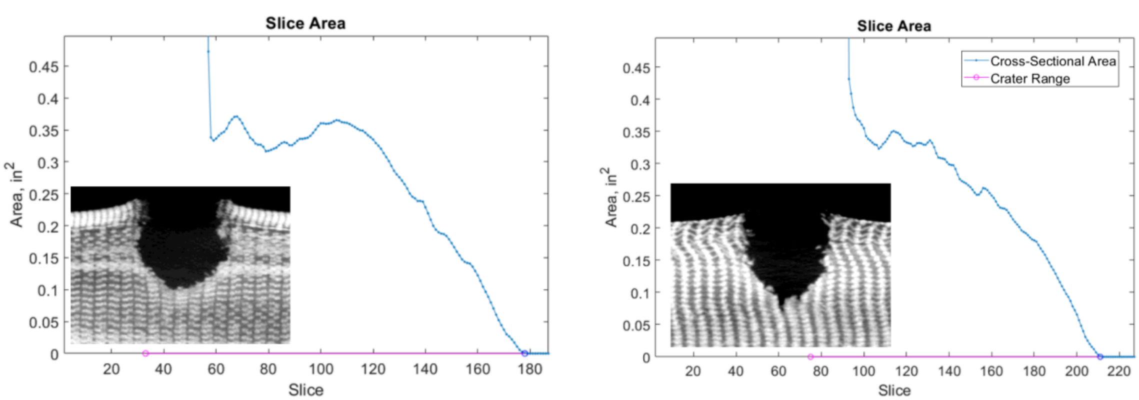

(a) (b)

Fig. 14. Example IMPACT cross-sectional area outputs of each slice in a HEEET HVIT CT scan. (a) 0.1” RL coupon profile (b) IL only coupon profile. Slice 0 notes the top of the scan, with the magenta bar along the x-axis showing IMPACT’s calculated crater depth range.

5 CONCLUSIONS AND FUTURE WORK

The FY19 HVI test series suggests that while increasing HEEET Recession Layer thickness does reduce crater depth somewhat, it is not a mass efficient mitigator of MMOD impact risk. Due to the EEV's tight mass constraint, this ultimately led to the recommendation of a HEEET Insulation Layer only forebody heat shield. Current analyses do not predict positive margins against failure for 1e-6 probability kinetic energy for thermally-designed TPS thickness. To mitigate this risk, further work is being done to understand the limitations of the environment models, and trade studies are being set up to assess both design changes to the vehicle itself and the effects of later release times of the EEV on the preceding stages of the MSR mission.

The results from this test program will be used to better characterize models of hypervelocity impact damage to dual-layer TPS. These results, including detailed analysis of material response and crater morphology, will be fed into coupled aerodynamic/thermal response models, which produce an overall risk of failure given a particular form of HVI damage. The capability of the IMPACT code developed at NASA ARC is central to this effort, as it allows analysis of damage progression to be performed on actual craters, rather than geometric approximations, better capturing sensitivities to crater morphology.

6 REFERENCES

1. Ellerby et al, *Heatshield for Extreme Entry Environment Technology (HEEET) Thermal Protection System (TPS)*, NASA Ames Research Center, Moffett Field, California, 2019.
2. Bjorkman, M.D., Christiansen, E.L. *Meteoroid and Orbital Debris (MMOD) Risk Assessment Status*, NASA Johnson Space Center, Houston, Texas, 2018.
3. Moorhead, A.V. *NASA Meteoroid Engineering Model (MEM) version 3*, NASA Marshall Space Flight Center, Huntsville, Alabama, 2019.
4. Bjorkman, M.D., Christiansen, E.L., Lear, D.M. *Bumper 3 Software User Manual*, NASA Johnson Space Center, Houston, Texas, 2014.
5. Anderson, B.J., Smith, R.E. *Natural Orbital Environment Guidelines for Use in Aerospace Vehicle Development*, NASA Marshall Space Flight Center, Huntsville, Alabama, 1994.
6. Christman et al, *Study of the Phenomena of Hypervelocity Impact*, GM Defense Research Laboratory, Santa Barbara, California, 1963.
7. Noble et al, *Ale3d: An arbitrary Lagrangian-Eulerian multi-physics code*. Lawrence Livermore National Lab (LLNL), Livermore, CA (United States), 2017.